Available online at www.sciencedirect.com
ScienceDirect
Procedia Computer Science 54 (2015) 491 – 500
Procedia Computer Science

Eleventh International Multi-Conference on Information Processing-2015 (IMCIP-2015)

Occlusion Invariant Palmprint Recognition with ULBP Histograms

Deepti Tamrakar and Pritee Khanna*

PDPM Indian Institute of Information Technology, Design and Manufacturing, Jabalpur, India

Abstract

This work presents a palmprint recognition approach based on the local distribution of uniform patterns. Preprocessing segments palmprint region from foreground of image as well as aligns the palmprint along the line between tips of middle finger and mid of wrist. Palmprint texture has line and wrinkles like features which are a type of uniform patterns. Uniform LBP (ULBP) refers to the pattern of uniform appearance with limited discontinuities. ULBP histograms are used as features to handle occlusion upto 36%. Experiments are performed on 400 classes of the PolyU 2D, 600 classes of CASIA and 150 classes of IIITDMJ palmprint database. Correct identification rates of 99.6% for normal palmprints and 99% for randomly occluded palmprints are obtained on PolyU 2D database.

Peer-review under responsibility of organizing committee of the Eleventh International Multi-Conference on Information Processing-2015 (IMCIP-2015)

Keywords: Uniform local binary pattern; Entropy; Chi-square distance; EER; Occlusion.

1. Introduction

During the past decade, personal authentication using palmprints has been extensively studied. Palmprint based authentication approaches have good properties, such as permanence, uniqueness, low cost acquisition, and high accuracy[1,2]. Capturing a palmprint image in an unconstrained environment makes it difficult to align in the same precise position, and hence brings forth the problems of occlusion, rotation, and translation (shift)[3]. Also, some portion of the palm may be suffered by occlusion due to misplacement or misalignment of the palmprint[4]. In the real life situations, it might be desirable to recognize a palm which may be partially occluded due to reasons like injury, tattoo, dust, or grease marks. Some example images are given in Fig. 1. In such situations a system is sought after, that is accustomed to recognize palmprint from occluded palm image with a good classification rate.

The proposed work aims to develop an efficient palmprint verification and identification system that performs well for normal (non-occluded) as well as occluded palmprint images. This requires palmprints alignment in the same precise position before ROI (Region of Interest) segmentation. The system uses small number of features and is robust against varying extents of occlusion.

The paper is organized as follows: Section 2. reviews some a few related palmprint feature extraction approaches. Section 3. describes the process flow of the proposed system. It also describes palmprints databases used for experiments, ROI extraction technique developed, feature extraction, and palmprint matching for the proposed system. Section 4. explains experimental setup and discusses performance of the proposed approach on non-occluded (normal) and occluded palmprints. Section 5. concludes the work.

*Corresponding author. Tel: +91-761-2632273. Fax: +91-761-2632524.
E-mail address: pkhanna@iiitdmj.ac.in

Peer-review under responsibility of organizing committee of the Eleventh International Multi-Conference on Information Processing-2015 (IMCIP-2015)
doi:10.1016/j.procs.2015.06.056

(a) (b) (c) (d)

Fig. 1. Some examples of occluded palmprints ((a)–(b)[5]).

2. Literature Review

Palmprint texture features are calculated by many techniques, such as Fourier transform[6], Gabor transform[3], Wavelet transform[7], Directional sub-band decomposition[8], Radon transform[9], Local Binary Pattern (LBP)[10,11], and many more[1,2]. These techniques rely on some unique invariant property which can be utilized to find the robust features. 2D Gabor transform outperforms for palmprint recognition due to its accurate spatial frequency localization, and robustness against varying brightness and contrast of images[3]. Gabor filter based texture coding methods, such as Comp code, Palm code, Fusion code and XOR-Sum code perform well for one-to-one matching of palmprints[2,12]. These methods are invariant to illumination but do not perform well even for a small rotation and shift. Image moments, such as Zernike, Legendre and Hu, have also been extracted from sub-images of palmprint ROI and used for palmprint recognition[4,13,14].

Some LBP-based palmprint recognition systems have been proposed with different machine learning techniques[15,16]. In literature LBP histograms extracted from scalable sub-windows are considered as features. Weighted Chi-square distance is used for palmprint matching and the weight of each sub-window is calculated by Adaboost learning[11,17]. However, these methods take long time to extract features because of increasing number of neighbors to determine LBP. In another approach, LBP descriptor is applied on four directional palmprint gradient responses given by sobel operator[18]. Each directional response is divided into 10 different sub-blocks and ULBP histogram of each block is used as feature vector. Modified probabilistic neural network (PNN) is used to match 2,360 features. In another work, ROI is decomposed into sub-bands with complex directional wavelet coefficients (CDFB) upto 3-levels; each sub-band is divided into sub-blocks; and ULBP histogram of each sub-block is calculated. Further, fisher linear discrimination is applied for dimension reduction[15]. Recent researches are focused on improving the quality of palmprint features against variations in position, rotation, scale, noise, translation, occlusion, and illumination[4,15,19,20]. To make a robust palmprint recognition system, two or more feature extraction techniques are essentially combined[15]. Some of the local texture descriptors, such as Scale Invariant Fast Transform (SIFT)[21,22], Speed Up Robust Feature (SURF)[23], and Zernike moments[4] are also employed for occluded palmprints.

LBP based methods are powerful but mainly focus on recognition of a normal palmprint without any variation present in it. This work proposes use of ULBP (Uniform Local Binary Pattern) histograms of palmprint ROI sub-images for occluded palmprint identification and verification. In literature some results are discussed for the same amount of occlusion present at the same portion in all test palmprints. But in the real life situation, as shown in Fig. 1, the size and position of occlusion on palmprint may vary. The present work takes care of randomly occluded palmprints, i.e., different amount of occlusion present at different positions in all test palmprints. However, system is trained with normal palmprints only.

3. Proposed Palmprint Recognition System

Figure 2 shows flow diagram of the proposed palmprint recognition system robust to occlusion. The process starts with palmprint image captured with a scanner or camera. The acquired palmprint image is preprocessed to extract the region of interest (ROI). This ROI is partitioned into sub-images, and ULBP histogram as discussed in Section 3.3 is calculated for each sub-image. Entropy of each sub-image is used to identify non-occluded sub-images in the test ROI. Matching is performed between corresponding features of non-occluded sub-images identified in test palmprint and enrolled palmprints. Matching distances of all non-occluded sub-images are fused with averaging sum rule to get the

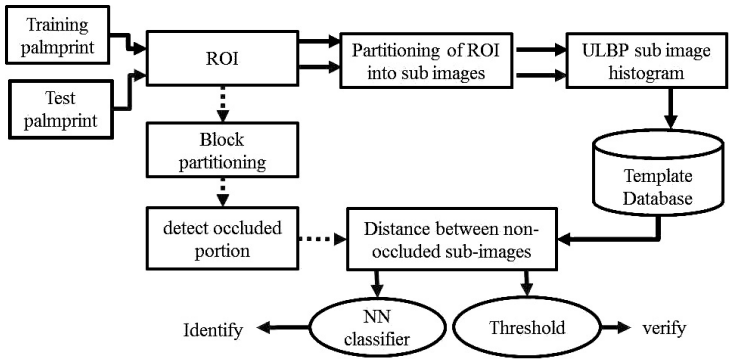

Fig. 2. Flow diagram of the proposed palmprint recognition system.

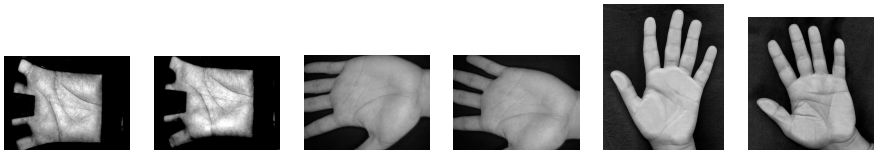

Fig. 3. (a)–(b) PolyU 2D (c)–(d) CASIA and (e)–(f) IIITDMJ palmprints.

final matching distance. Test palmprint verification is performed with some predefined threshold, while the Nearest Neighbor (NN) classifier is used for identification.

3.1 Palmprint databases

Effectiveness of the proposed system is evaluated on three palmprint databases, PolyU 2D[24], CASIA[25], and a self collected IIITDMJ database. Acquisition devices and the number of palmprints are different in these databases. As compared to PolyU 2D, the palmprint images in CASIA and IIITDMJ databases suffer more from palm movements and distortion. Figure 3 shows two palmprint samples from each database. PolyU 2D palmprint database consists of 8,000 gray scale images (384 $\times$ 284) obtained from 400 different palms of 200 users. 10 images of left and right palmprints were collected with a 75 dpi CCD scanner at an interval of around two months. CASIA Palmprint database contains 5,335 gray scale palmprint images (640 $\times$ 480 pixels, 72 dpi) collected from 312 individuals in a single session using CMOS camera. This setup imposes less physical constraints on the users palm as compared to PolyU capturing device, and hence leads to palm movements introducing distortions and blurring in the captured palmprint images. 900 gray scale palmprint images are collected from 75 students of IIITDM Jabalpur (Six images per palm) during one session and referred as IIITDMJ palmprint database here. The acquisition device is kept constraint free for rotation and translation to appear.

3.2 Preprocessing

Textural information present in the center part of a palm can be used to discriminate palms. ROI segmentation is also important for efficient feature extraction. ROIs of palmprints are mostly extracted in five basic steps: Gaussian filtering, binarization, boundary tracking, building coordinate, and ROI cropping. Preprocessing segments palmprint region from foreground of image as well as aligns the palmprint along the line between tips of middle finger and mid of wrist. PolyU 2D palmprints are captured in a constraint environment and their ROIs are extracted with a technique earlier proposed by us[26]. CASIA palmprints are collected from different distance and position between hand and camera, while IIITDMJ palmprints are collected from a scanner with a fixed resolution. Due to different size of hand

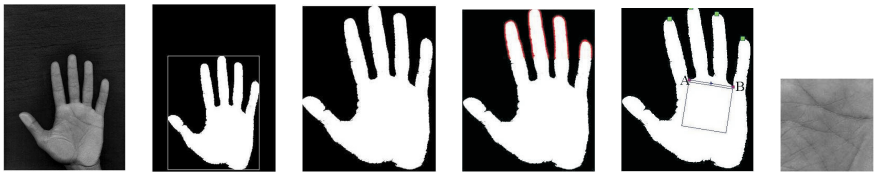

Fig. 4. ROI extraction (a) original palmprint; (b) binarization; (c) palmprint alignment; (d) finger boundary extraction; (e) coordinate alignment; (f) extracted ROI.

of each person, ROIs of different sizes are segmented from these databases. The following steps are followed to extract ROIs from CASIA and IIITDMJ images (Fig. 4):

1. To segment the palmprint region from the background image, gray scale palmprint image is converted into binary image by using a threshold obtained by local minima of palmprint histogram[26]. Irrelevant parts of this binary image are removed by morphological open operations.
2. Palmprint is segmented by bounding box operation on the mask of the region having the maximum area in the binary images. So obtained segmented image is rotated perpendicular to the maximum elliptical axis, which is a line between tip of the middle finger and mid of the wrist[8].
3. Boundary of four fingers is extracted by tracing the boundary pixel of palmprint segment from top left to right bottom, while limiting the height of the fingers to one third height of the palmprint image.
4. Tips of four fingers are selected on the basis of local maximum of y coordinate on the boundary pixels of fingers. Similarly, the gap between two fingers, labeled as A and B is obtained through the local minimum of the boundary pixels between tips of two fingers.
5. A square region of size AB drawn parallel to line AB at a distance of one-tenth of AB is ROI.

3.3 Uniform local binary pattern histogram of sub-images as feature

LBP is a powerful operator used for discrimination of gray-scale texture, which characterizes the spatial structure of the local image texture[16]. Consider a central pixel $g_c(x_c, y_c)$ in the image. The LBP (P, R) operator is defined as the binary difference between the gray value of a pixel $g_c(x_c, y_c)$ and the gray values of its P neighborhood placed on a circle of radius R:

$$\mathrm{LBP}(P, R) = \sum_{p=0}^{p=P-1} s(g_c - g_p)2^p \ \text{ where } \ s(x) = \begin{cases} 1 & x \geq 0; \\ 0 & x < 0. \end{cases} \tag{1}$$

The coordinates of the neighbors g_p are given by $(x_c + R\cos(2\pi p/P), y_c + R\sin(2\pi p/P))$. The sampling points that do not fall within the pixels are interpolated using bi-linear interpolation. The LBP (P, R) operator produces 2^P different output values corresponding to 2^P different binary patterns formed by the P pixels in the neighbor set. The corresponding decimal value of the generated binary number is used for labeling the given pixel. A uniformity measure, U of an LBP is defined as the number of spatial transition (bitwise 0/1) in that pattern, given as:

$$U = s(g_{P-1} - g_c) - s(g_1 - g_c)| + \sum_{p=1}^{P-1} |s(g_p - g_c) - s(g_{p-1} - g_c)| \tag{2}$$

The uniform patterns are denoted by ULBP(P, R) and defined by the Eqn. 3. ULBP(P, R) contains maximum two bitwise transitions from 0 to 1 or vice versa when the binary string is considered circular ($U \leq 2$). For example, the value of U for LBP patterns 00000000 and 01000000 is 0 and 2, respectively.

$$\mathrm{ULBP}(P, R) = \begin{cases} \sum_{p=0}^{p=P-1} s(g_c - g_p)2^p & \text{if } U \leq 2; \\ P(P-1) + 2 & \text{otherwise.} \end{cases} \tag{3}$$

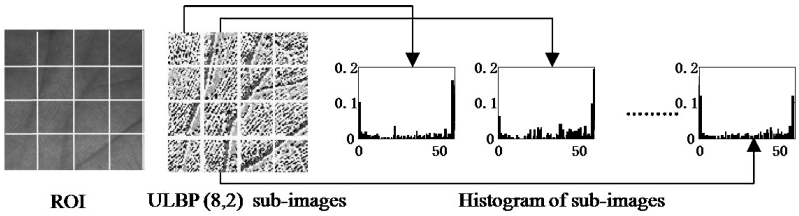

Fig. 5. Feature extraction from ROI.

The uniform LBP (ULBP) refers to the pattern of uniform appearance, which has limited transition or discontinuities. ULBP contain about 90% information of local micro-patterns, such as edges, spots, and flat areas of a natural image. Uniform patterns are statistically more stable and less prone to noise than LBP[10,27]. Palmprint texture has line and wrinkles like feature which are a type of uniform pattern. Histograms of LBP and ULBP images are very powerful texture features as they contain information of the distribution of local micro-patterns, such as edges, spots, and flat areas. When uniform patterns are used in the computation of the ULBP histogram, each uniform pattern is assigned a separate bin whereas the non-uniform patterns are assigned a single bin. Therefore, the total number of bins for LBP histograms is 2^P, while the total number of bins for ULBP histograms is $P(P-1)+3$. For example, the number of bins for LBP(8, R) is 256, but are only 59 for ULBP(8, R). In view of this, ULBP histograms are considered as the feature vector of the palmprints in the present work.

The extracted ROI is divided into $M \times M$ sub-images. ULBP histogram of each sub-image is considered as its feature. Time complexity as well as the size of feature vector increases with increasing values of P in ULBP. ULBP(8, 1) and ULBP(8, 2) provide good texture information and are considered in this work. Figure 5 demonstrates the partition of ROI into $4 \times 4 = 16$ sub-images, corresponding ULBP image and concatenated histogram of the block images.

3.4 Use of entropy to handle palmprint occlusion

The proposed system uses ULBP histogram from the non-occluded sub-images of ROI as the features. The extracted ULBP histogram of a sub-image is independent to that of other sub-images. Hence, the system can be made robust to occlusion. Since palmprints are rich in texture, the randomness of palmprint sub-images should also be high. Entropy is a statistical measure of randomness that can be used to characterize the occluded parts in images. The randomness in the occluded sub-image would be low as there is less texture information as compared to the non-occluded sub-image. As a result, the entropy of the occluded part is always less than the non-occluded part. During testing, the occluded parts in the ROI are detected on the basis of entropy and a predetermined threshold. The threshold is calculated during the training phase of the system. While training, entropy of $(i, j)^{\text{th}}$ sub-image of T^{th} template is calculated as

$$E_T(i,j) = -\sum_{b=1}^{b=B} T_{i,j,b} \log_2 T_{i,j,b} \tag{4}$$

where B represents gray levels and $T_{i,j,b}$ is the probability of $(i, j)^{\text{th}}$ sub-image having b^{th} gray level. Also, average entropy of each $(i, j)^{\text{th}}$ sub-image of all training images (N_T) are calculated as

$$AE(i,j) = \frac{1}{N_T} \sum_{T=1}^{N_T} E_T(i,j) \tag{5}$$

The average entropy of each sub-image is treated as the threshold to identify corresponding sub-images of the query image as occluded or non-occluded during testing phase.

$$\text{Occ}(i,j) = \begin{cases} 1; & E_Q(i,j) \geq 0.8 * \text{AE}(i,j) \\ 0; & E_Q(i,j) < 0.8 * \text{AE}(i,j) \end{cases} \tag{6}$$

If $\mathrm{Occ}(i, j)$ of (i, j) sub-image is 1 then it is considered non-occluded, otherwise occluded. Weight W for each $M \times M$ sub-image of query ROI is calculated as

$$W(i, j) = \frac{\mathrm{Occ}(i, j)}{\sum_{i=1}^{M} \sum_{j=1}^{M} \mathrm{Occ}(i, j)} \tag{7}$$

Features of occluded sub-images are not considered during matching. Palmprints match score $D(T, Q)$ is calculated as the average of Chi-square distances between non-occluded sub-images of query image Q and corresponding sub-images of stored template T as

$$D(T, Q) = \frac{1}{B} \sum_{i=1}^{M} \sum_{j=1}^{M} W(i, j) \sum_{b=1}^{B} \frac{(T_{i,j,b} - Q_{i,j,b})^2}{T_{i,j,b} + Q_{i,j,b}} \tag{8}$$

where $T_{i,j,b}$ and $Q_{i,j,b}$ are normalized histogram of b^{th} ULBP value in (i, j) sub-image.

4. Experimental Setup and Results

The robustness of the proposed approach is tested on normal and artificially occluded palmprints. Performance of the proposed system is evaluated on Intel Quad Core processor @2.83 GHz with 8 GB RAM. All simulations are performed using MATLAB®. The details of palmprints used in training and testing phases are given in Table 1.

The performance of the proposed palmprint recognition system is measured on the basis of Equal Error Rate (EER), Decidability Index (DI), Correct Identification Rate (CIR) and Receiver Operating Characteristics (ROC) curves. ROC curve is the visual characterization of the plot between False Acceptance Rate (FAR) and False Rejection Rate (FRR). EER is a crossover point of the FAR and FRR. DI is a good measure to calculate separability of genuine and impostor classes. A biometric recognition system must have DI and CIR as high as possible while the value of EER should be as small as possible.

4.1 Finding suitable number of sub-images

The proposed system works on the similarity between corresponding non-occluded blocks of query image and stored template. If the number of partitions of palmprint are less, a large region of palmprint would be omitted for small occlusion. To avoid omission of non-occluded region from matching, the palmprint is expected to partition into many sub-images. Increasing the number of sub-images makes recognition processes computationally expensive, hence suitable number of partitions giving good performance are supposed to be obtained. Entropy of the sub-image is a measure of its texture information. Figure 6 shows that the mean entropy of the sub-images of ROI decreases with increasing number of ROI partitions due to reduction in the size of sub-images. Discrimination of texture becomes difficult with much smaller size of sub-image obtained through increasing number of partitions. To obtain suitable number of sub-images palmprint ROIs are partitioned into 1×1 to 8×8 number of sub-images and their performance is analyzed.

4.2 Testing on normal palmprints

It has been reported that ULBP(8, 1) and ULBP(8, 2) contain almost 90% of all pattern for texture images[16]. Increased number of neighbors to calculate ULBP histograms increases the size of feature vector as well as the

Table 1. Distribution of palmprint images.

Database	Total palmprints	Palms	Palmprints/Palms	Training palmprints/palm	Test palmprints/palm
PolyU	8,000	400	20	5	15
CASIA	5,335	624	≈8	2	6
IIITDMJ	900	150	6	2	4

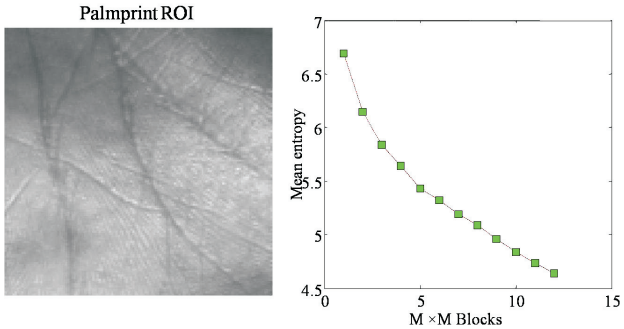

Fig. 6. (a) ROI (b) Plot between number of sub-images and their mean entropy for PolyU 2D.

Table 2. Experimental results obtained with ULBP(8, 1) and ULBP(8, 2) for different number of sub-images of normal palmprints.

		ULBP(8, 1)			ULBP(8, 2)		
Database	No. of partitions	EER(%)	DI	CIR(%)	EER(%)	DI	CIR(%)
PolyU 2D	1 × 1	11.52	1.81	59.10	11.49	1.82	63.83
	2 × 2	6.85	2.47	88.53	6.80	2.50	91.48
	3 × 3	5.03	2.94	95.15	4.51	3.03	97.20
	4 × 4	3.59	3.39	97.30	3.18	3.51	98.45
	5 × 5	2.63	3.79	98.62	2.35	3.93	99.10
	6 × 6	1.90	4.08	99.03	2.03	4.17	99.58
	7 × 7	**1.56**	**4.34**	**99.43**	**2.02**	**4.32**	**99.60**
	8 × 8	1.63	4.38	99.28	2.22	4.34	99.47
CASIA	1 × 1	10.20	1.56	41.92	8.87	1.70	58.80
	2 × 2	6.66	1.93	82.59	5.95	2.07	88.74
	3 × 3	5.52	2.35	91.44	4.85	2.60	94.22
	4 × 4	**4.66**	**2.69**	**94.50**	**4.35**	**2.90**	**95.38**
	5 × 5	5.35	2.81	94.15	4.82	3.11	95.31
	6 × 6	5.66	2.98	94.25	5.17	3.20	94.98
	7 × 7	6.13	3.01	93.66	5.81	3.15	94.39
	8 × 8	8.82	3.01	93.26	6.39	3.08	93.33
IITDMJ	1 × 1	6.05	2.05	90.31	5.73	2.10	92.07
	2 × 2	2.71	3.21	95.59	2.90	3.15	98.24
	3 × 3	2.20	3.79	98.68	2.20	3.90	99.12
	4 × 4	**1.16**	**4.18**	**99.56**	**1.61**	**4.34**	**100**
	5 × 5	1.76	4.43	99.12	1.32	4.86	99.12
	6 × 6	1.76	4.63	98.68	1.32	5.00	98.68
	7 × 7	1.76	4.82	98.68	1.76	5.04	98.68
	8 × 8	1.76	4.82	98.68	1.76	5.15	98.24

computation time. Performance of the proposed approach is tested on normal palmprints for ULBP(8, 1) and ULBP(8, 2) with different number of partitions to find suitable combination of partition size $M \times M$ and neighborhood radius R. Table 2 gives the performance in terms of EER, DI and CIR for all three palmprint databases.

It is found that performance of the system improves with increasing number of sub-images but up to a specific partition, i.e., 7×7 partitions for PolyU 2D and 4×4 partitions for CASIA and IIITDMJ databases. The reason behind this difference is the fact that the quality of palmprint images in CASIA and IIITDMJ databases is low as compared to PolyU 2D database, which seizes the texture discrimination beyond 4×4 partitions also, but the performance degrades beyond 7×7 partitions. DI improves with the increasing number of ROI partitions, as it depends on the size of features. Performance parameters, i.e., feature size, and computation time of feature extraction and matching are proportional to number of sub-image partitions. The system may be fine tuned as per the performance requirement.

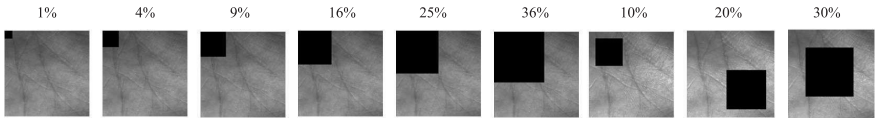

Fig. 7. Examples of artificially occluded ROIs.

Table 3. Experimental results on occluded test palmprints.

			ULBP(8, 1)			ULBP(8, 2)		
Database	No. of partitions	occ (%)	EER(%)	DI	CIR(%)	EER(%)	DI	CIR(%)
PolyU 2D	(7 × 7)	0	1.56	4.34	99.43	2.02	4.32	99.60
		1	1.74	4.34	99.37	2.05	4.32	99.57
		4	1.86	4.31	99.32	2.20	4.25	99.40
		9	1.97	4.29	99.22	2.50	4.07	99.10
		16	2.09	4.25	99.15	3.58	3.71	98.00
		25	2.35	4.25	99.08	6.76	3.00	95.45
		36	2.82	4.25	98.72	7.04	2.97	83.07
CASIA	(4 × 4)	0	4.66	2.69	94.50	4.35	2.90	95.38
		1	5.38	2.67	93.38	4.59	2.88	94.32
		4	5.51	2.58	92.70	4.60	2.71	93.96
		9	5.92	2.57	89.49	5.53	2.68	91.32
		16	8.52	2.33	78.97	7.90	2.35	88.54
		25	8.71	2.27	74.13	9.56	2.17	83.82
		36	9.69	2.25	60.89	14.56	1.75	58.82
IIITDMJ	(4 × 4)	0	1.16	4.18	99.56	1.61	4.34	100
		1	1.25	4.17	99.56	1.69	4.25	99.12
		4	1.27	4.13	99.56	1.62	4.23	99.12
		9	1.54	4.10	99.30	1.76	4.14	99.12
		16	1.71	3.51	98.30	1.76	4.09	99.12
		25	2.74	3.96	97.56	3.77	4.41	96.92
		36	3.52	3.35	93.83	2.64	3.87	96.92

4.3 Testing on artificially occluded palmprints

To evaluate the robustness of the proposed approach against occlusion, the templates of normal palmprint are used for training in the way described in Section 4. and occluded palmprint are used for testing. Two sets of experiments are performed with artificially introduced occlusion up to 36% as shown in Fig. 7.

Experiment 1: Fixed size occlusion Table 3 shows performance of the proposed approach on artificially occluded test ROIs with fixed size of occlusion from upper-left corner of the ROI for all three palmprint databases. It has been observed that occlusion upto 36% does not affect the parameters significantly. However, the performance degrades with increasing radius for higher amount of occlusion.

Experiment 2: Random occlusion In real life, the size and position of occlusion in palmprints vary for different reasons. Some examples of palmprints having natural occlusion due to injury and tattoo are already shown in Fig. 1. As the database of naturally occluded palmprints is not yet available publicly, the proposed method is validated on artificially occluded test ROIs with occlusion upto 30% introduced at any portion on it. The testing is done five times on each combination of the setup and the performance measures are taken as average values. Table 4 compares the performance of proposed approach for randomly occluded palmprints. The number of partitions are initially selected on the basis of the best performance observed for normal palmprints. For PolyU 2D, the best results are already obtained for 7×7 partitions which is also suitable for the occluded sub-images. However, the performance for normal images of CASIA and IIITDMJ databases is found better for 4×4 partitions but it degrades drastically for randomly

Table 4. Experimental results for randomly occluded palmprint.

			ULBP(8, 1)			ULBP(8, 2)		
Database	No. of partitions	Type of palmprint	EER(%)	DI	CIR(%)	EER(%)	DI	CIR(%)
PolyU 2D	7×7	Normal	1.56	4.34	99.43	2.02	4.32	99.60
		Occluded	2.37	4.09	99.18	2.94	3.74	99.00
CASIA	4×4	Normal	4.66	2.69	94.50	4.35	2.90	95.38
		occluded	9.81	2.20	92.84	5.74	3.18	94.54
	7×7	Normal	6.13	3.01	93.66	5.81	3.15	94.39
		Occluded	6.71	2.94	93.64	5.73	3.18	94.54
IIITDMJ	4×4	Normal	1.16	4.18	99.56	1.61	4.34	100.00
		Occluded	4.07	3.44	99.61	1.80	3.98	100.00
	7×7	Normal	1.76	4.82	98.68	1.76	5.15	98.68
		Occluded	1.80	4.64	98.68	1.76	5.02	98.62

Table 5. Comparisons with other LBP based approaches for PolyU 2D palmprint database.

Reference	Guo *et al.* 2010[11]	Mu *et al.* 2011[15]	Proposed approach
Histogram bin length	5568	6254	2891
Size of feature vector	5568	385	2891
Learner	NA	FLD	NA
EER	NA	NA	1.56
CIR	99.67%	93.31%	99.60%

NA: Information not available.

occluded palmprints. Therefore, randomly occluded palmprints of CASIA and IIITDMJ database are also tested for 7×7 partitions. It also shows that the partition size should be sufficiently large to handle occlusion.

4.4 Comparisons with other methods

PolyU 2D palmprint database is a standard database publicly available. Therefore, the proposed approach is compared with the existing methods for PolyU 2D. Table 5 shows that the performance of the proposed ULBP based palmprint recognition system is better than other LBP-based approaches. The hierarchical multi-scale LBP[11] uses non-uniform patterns for three radius ($R = 2, 3, 4$) with ROI partitions into 4×4 sub-blocks. This method performs well but the size of feature vector is very large. In another work ULBP histogram is calculated from sub-block of CDFB coefficients and the size of feature vector is reduced by Fisher Linear Discrimination (FLD)[15]. These methods are suitable for palmprint identification, and therefore the results are compared in terms of CIR. The proposed approach achieves CIR upto 99.6% with 7×7 partitions, which is very close to the hierarchical multi-scale LBP approach[11].

5. Conclusions

This paper presents an efficient system for palmprint verification and identification which is invariant to occlusion. ROI extraction makes the system invariant to size and rotation of the palm. The uniform patterns are statistically robust and less prone to noise and illumination. The variation in the size of ROI is tackled by considering ULBP histograms as the feature vector. A sub-image is classified as occluded or non-occluded on the basis of average entropy of corresponding sub-images of training set. Only non-occluded sub-images are considered to calculated the normalized match score between two palmprints. The number of ROI partitions can be chosen as per system requirements. Experiments on three palmprint databases reveals that 4×4 partitions of ROI can handle recognition of normal palmprint but to tackle the occluded palmprints efficiently, the partition size should be sufficiently large. More than 7×7 sub-images partitions with ULBP(8, 1) better performs on ROIs occluded upto 36% as well as naturally occluded ROIs.

References

[1] A. Kong, D. Zhang and M. Kamel, A Survey of Palmprint Recognition, *Pattern Recognition*, vol. 42(7), pp. 1408-1418, (2009).

[2] D. Zhang, W. Zuo and F. Yue, A Comparative Study of Palmprint Recognition Algorithms, *ACM Computing Surveys (CSUR)*, vol. 44(1), pp. 2, (2012).

[3] X. Pan and Q. Q. Ruan, Palmprint Recognition using Gabor-Based Local Invariant Features, *Neurocomputing*, vol. 72(7), pp. 2040-2045, (2009).

[4] G. Badrinath, N. K. Kachhi and P. Gupta, Verification System Robust to Occlusion using Low-Order Zernike Moments of Palmprint Sub-Images, *Telecommunication Systems*, vol. 47(3–4), pp. 275-290, (2011).

[5] Google Images, http://www.google.com/imghp, (2014). [Online; accessed July-2014].

[6] W. Li, D. Zhang and Z. Xu, Palmprint Identification by Fourier Transform, *International Journal of Pattern Recognition and Artificial Intelligence*, vol. 16(04), pp. 417-432, (2002).

[7] H. Imtiaz and S. A. Fattah, A Wavelet-based Dominant Feature Extraction Algorithm for Palmprint Recognition, *Digital Signal Processing*, (2012).

[8] A. B. Mansoor, H. Masood, M. Mumtaz and S. A. Khan, A Feature Level Multimodal Approach for Palmprint Identification using Directional Subband Energies, *Journal of Network and Computer Applications*, vol. 34(1), pp. 159-171, (2011).

[9] W. Jia, D. S. Huang and D. Zhang, Palmprint Verification based on Robust Line Orientation Code, *Pattern Recognition*, vol. 41(5), pp. 1504-1513, (2008).

[10] Y. Zhao, W. Jia, R. Hu and J. Gui, Palmprint Identification using LBP and Different Representations, In *International Conference on Hand-Based Biometrics (ICHB) IEEE*, pp. 1-5, (2011).

[11] Z. Guo, L. Zhang, D. Zhang and X. Mou, Hierarchical Multiscale LBP for Face and Palmprint Recognition, In *17th IEEE International Conference on Image Processing (ICIP), IEEE*, pp. 4521-4524, (2010).

[12] D. Tamrakar and P. Khanna, Palmprint Verification with Xor-Sum Code, *Signal, Image and Video Processing*, vol. 9(3), pp. 535-542, (2015).

[13] J. S. Noh, and K. H. Rhee, Palmprint Identification Algorithm using Hu Invariant Moments and Otsu Binarization, In *Fourth Annual ACIS International Conference on Computer and Information Science, IEEE*, pp. 94-99, (2005).

[14] C. L. Deepika, A. Kandaswamy, C. Vimal and B. Satish, Palmprint Authentication using Modified Legendre Moments, *Procedia Computer Science*, doi:http://dx.doi.org/10.1016/j.procs.2010.11.021; Proceedings of the International Conference and Exhibition on Biometrics Technology, vol. 2, pp. 164-172, (2010).

[15] M. Mu, Q. Ruan and S. Guo, Shift and Gray Scale Invariant Features for Palmprint Identification using Complex Directional Wavelet and Local Binary Pattern, *Neurocomputing*, vol. 74(17), pp. 3351-3360, (2011).

[16] T. Ojala, M. Pietikainen and T. Maenpaa, Multiresolution Gray-Scale and Rotation Invariant Texture Classification with Local Binary Patterns, *IEEE Transactions on Pattern Analysis and Machine Intelligence*, vol. 24(7), pp. 971-987, (2002).

[17] X. Wang, H. Gong, H. Zhang, B. Li and Z. Zhuang, Palmprint Identification using Boosting Local Binary Pattern, In *18th International Conference on Pattern Recognition, IEEE*, vol. 3, pp. 503-506, (2006).

[18] G. K. Ong Michael, T. Connie and A. B. Jin Teoh, Touch-Less Palm Print Biometrics: Novel Design and Implementation, *Image and Vision Computing*, vol. 26(12), pp. 1551-1560, (2008).

[19] G. Badrinath and P. Gupta, Robust Biometric System using Palmprint for Personal Verification, *Advances in Biometrics*, pp. 554-565, (2009).

[20] G. Badrinath and P. Gupta, Palmprint based Recognition System using Phase-Difference Information, *Future Generation Computer Systems*, vol. 28(1), pp. 287-305, (2012).

[21] G. Badrinath and P. Gupta, Palmprint based Verification System Robust to Rotation, Scale and Occlusion, In *12th IEEE International Conference on Computers and Information Technology, IEEE*, pp. 408-413, (2009).

[22] J. Chen and Y. S. Moon, Using Sift Features in Palmprint Authentication, In *19th International Conference on Pattern Recognition, IEEE*, p. 1-4, (2008).

[23] G. Badrinath, P. Gupta and H. Mehrotra, Score Level Fusion of Voting Strategy of Geometric Hashing and Surf for an Efficient Palmprint-Based Identification, *Journal of Real-Time Image Processing*, pp. 1-20, (2011).

[24] D. Zhang, Polyu Palmprint Database, Biometric Research Centre, Hong Kong Polytechnic University, Available online at http://www.comp.polyu.edu.hk/biometrics, (1998).

[25] Z. S. Tieniu Tan, Casia Palmprint Database, http://biometrics.idealtest.org/ (2005).

[26] D. Tamrakar and P. Khanna, Analysis of Palmprint Verification using Wavelet Filter and Competitive Code, In *International Conference on Computational Intelligence and Communication Networks (CICN), 2010 IEEE*, pp. 20-25, (2010).

[27] J. Ren, X., Jiang and J. Yuan, Noise-Resistant Local Binary Pattern with an Embedded Error-Correction Mechanism, *IEEE Transactions on Image Processing*, vol. 22(10), pp. 4049-4060, (2013).